"Real museums are places where Time is transformed into spaces"

Orhan Pamuk in "The Museum of Innocence"

5

Neutrino phenomenology with S_4 flavor symmetry in inverse and type II seesaw

---

In this chapter we have exercised an inverse seesaw model based on the S_4 flavor symmetry with an adaptation of type II seesaw mechanism. The leading order neutrino mass is explained under the scheme of ISS, which is later on accompanied by the type II seesaw mechanism in order to reproduce non-zero reactor mixing angle. The type II seesaw perturbation at the same time yields the other oscillation parameters undeviated from their correct 3σ range. A detailed analysis has been performed by varying the Dirac Yukawa coupling and type II seesaw strength which together play a crucial role in obtaining the oscillation parameters in agreement with the recent experiments. We calculate the contribution to the effective mass governing $0\nu\beta\beta$ decay assuming it to take place through the exchange of light neutrinos.

5.1 Introduction

On 4th of July 2012, there was a milestone discovery by the ATLAS and CMS collaborations at the CERN Large Hadron Collider (LHC), of the last missing entity of the standard model of particle physics i.e., the Higgs Boson which is electrically neutral and said to have a mass around 125 GeV. Till date this discovery seems to complete the menagerie of the particles of the SM and can address many observable phenomena of the SM. In addition this discovery also gave a concrete explanation of the elementary particles getting masses by interacting with the Higgs Boson. However the SM in spite of this new discovery is unable to address many issues. Existence of tiny neutrino mass and its large mixing angles is one such observation which the SM is unable to account for.

There has been several theoretical models proposed so far, in order to investigate the neutrino oscillation parameters in detail. After the announcement made by T2K [1] and RENO [2] and Daya Bay [3] the reactor mixing angle also gained very much interest in recent years. In this context a class of particle physics models have been suggested explaining the origin of non-zero reactor angle at the same time keeping other neutrino oscillation parameters consistent with experiments. In the neutrino sector also there are several issues which are yet to be addressed like which hierarchy pattern the neutrino mass follows, then the octant of the atmospheric mixing angle and finally, whether neutrino is a Dirac or Majorana particle. Neutrino less double beta decay is considered as the most profound evidence in support of the Majorana nature of the neutrino. All of these puzzles motivate us to extend the SM particle sector which we generally call as a SM extension.

As reported by many observations and experiments which are dedicated to neutrino oscillation phenomena, it is a well established fact that neutrinos are massive, however small there mass is. This fact demands a justification from the point of theoretical model building. We know that for the explanation of non zero neutrino mass one needs to go BSM. This journey starts with inclusion of SM scalar and fermion sector. The fermion sector is extended with a number of right handed gauge singlets which after coupling with left handed lepton doublets

and SM Higgs, seem to generate neutrino mass. This whole scenario is mathematically realized via the implementation of Weinberg's Dimension 5 operator [4, 5], which beautifully explains the nonzero neutrino mass without a fine tuning of the Yukawa coupling. Inclusion of RH gauge singlets or RH neutrinos (RHN) in the standard model helps to explain the tiny neutrino mass with the help of Weinberg's operator in the frame work of type I seesaw mechanism. Generally type I seesaw indicates the RHN mass scale to be around 10^{15} to 10^{16} GeV, which is quite high in comparison to the present accessible energy status of the LHC and other particle accelerators. In this situation inverse seesaw (ISS) mechanism gives a road map connecting light neutrino mass to such a RHN mass scale which may be accessible at the colliders in near future. In this work we have studied an ISS scheme described by the authors in [6]. The ISS presents the explanation for sub-eV neutrino mass by means of keeping the RHN mass around few TeV. We also adopt type II seesaw mechanism in order to reproduce non-vanishing reactor angle. With this motivation of studying the oscillation parameters we proceed towards building an ISS and type II based model adopting the S_4 flavor symmetry group.

Having set the stage with so many RHNs it may be a ground for the search of Neutrinoless double decay (NDBD) which crucially involves RHNs. NDBD process is a distinctive probe for the determination of Majorana nature of neutrinos. This is a process which has non-trivial implications for particle physics and cosmology, although its observation still remained elusive. The search for this process constitutes another new province of neutrino physics permitting us to look for possible CP violation effects in lepton number violating processes. With this motivation in the light of the presented model we have also studied the effective mass prediction to neutrinoless double beta decay assuming it to take place via to light neutrino exchanges.

This chapter is organized as follows. In Section. 5.2 we present the ISS model with type II seesaw. Section. 5.3 has been dedicated for neutrinoless double beta decay. In Section. 5.4 is kept for numerical analysis. We discuss the results in Section. 5.5. Finally, in Section. 5.6 we end up with our conclusion.

5.2 Structure of the model

As already mentioned in the earlier chapters the ISS scheme manifests in addressing a sub-eV neutrino mass scale at the cost of proposing the RHN mass at a scale much lower than that associated with the Type I seesaw [7–12]. If we recall the ISS Lagrangian it goes like as follows.

$$\mathcal{L} = -\bar{\nu}_L m_D \nu_R - \bar{S}_L M \nu_R - \frac{1}{2}\bar{S}_L \mu S_L^C + \text{H.}C.. \tag{5.2.1}$$

The ISS model contains a pair of two gauge singlet leptons, ν_R and S respectively. μ is the lepton number violating scale here, which plays a non-trivial role in this seesaw scheme. The fact that if μ takes a zero value, then the lepton number symmetry is preserved , leading to a vanishing light neutrino mass. This fact demands a nonzero μ scale to bring a non-zero light neutrino mass. The scale of μ adds a new dimension in the mass generation mechanism of light neutrinos via accommodating a TeV scale RHN. This feature makes the ISS unique among all the seesaw schemes. Essentially the scale of the lepton number violating parameter μ is of order keV for an electro-weak scale Dirac neutrino mass m_D. In this scheme the effective light neutrino mass is obtained from the following equation.

$$m_\nu^I = m_D^T (M^T)^{-1} \mu M^{-1} m_D, \tag{5.2.2}$$

In this work Eq. (5.2.2) decides the structure of the leading order light neutrino mass. To implement the ISS scheme and to get a desired light neutrino mass structure we extend the SM scalar structure with the inclusion of five flavons which transform as singlets and one additional Higgs η transforming as doublet under $SU(2)$ symmetry group. Three right handed gauge singlets ν_R are introduced, which are supposed to transform as a triplet 3_1 of S_4. We assign the SM type Higgs η to the triplet 3_1 of S_4. The additional three SM fermion singlets 'S_i' are assumed to transform as an S_4 triplet 3_1. The charge assignments of the particle content of the model is presented in Table 5.1.

The Yukawa Lagrangian relevant for the above particle content is given by,

$$\mathcal{L}^I = y_D \bar{L} \nu_R \eta + y_D{}' \bar{L} \nu_R h + y_M \nu_R S \Phi_R + y_s S S \Phi_s, \tag{5.2.3}$$

	$\bar{L}$	ν_R	l_R	h	η	S	Φ_R	Φ_s	Φ_l	$\Phi_l{}'$	$\Phi_l{}''$
$SU(2)_L$	2	1	1	2	2	1	1	1	1	1	1
S_4	3_1	3_1	3_1	1_1	3_1	3_1	1_1	1_1	3_1	3_2	1_1
Z_2	+	-	+	-	-	-	+	+	+	+	+

Table 5.1: Fields and their transformation properties under $SU(2)_L$, the S_4 flavor symmetry and Z_2 flavor symmetry

The following flavon alignments help us to get a desired neutrino mass matrix.

$$\langle \Phi_R \rangle = v_R,\ \langle \Phi_s \rangle = v_s,\ \langle h \rangle = v_h,\ \langle \eta \rangle = v_\eta(1,0,0).$$

Decomposition of the various terms present in the Eq. (5.2.3) into singlets following the S_4 rules mentioned in Section 1.8 of Chapter 1 (for detail please see [13]), has been shown as follows

$$\begin{aligned} y_D \bar{L}_i \nu_{jR} \eta &= y_D[(L_2\nu_{3R} + L_3\nu_{2R})\eta_1 + (L_1\nu_{3R} + L_3\nu_{1R})\eta_2 + (L_2\nu_{1R} + L_1\nu_{2R})\eta_3] \\ &= y_D(L_2\nu_{3R} + L_3\nu_{2R})v_\eta, \\ y_D{}' \bar{L}_i \nu_{jR} h &= y_D{}'(L_1\nu_{1R} + L_2\nu_{2R} + L_3\nu_{3R})v_h, \end{aligned}$$

$$\begin{aligned} y_M \nu_{iR} S_j \Phi_R &= y_M(S_1\nu_{1R} + S_2\nu_{2R} + S_3\nu_{3R})v_R, \\ y_s S S \Phi_s &= y_s(S_1S_1 + S_2S_2 + S_3S_3)v_s. \end{aligned}$$

With the help of the S_4 product rules and using the chosen flavon alignments mentioned above we can design the following mass matrices.

$$m_D = y \begin{pmatrix} v_h & 0 & 0 \\ 0 & v_h & v_\eta \\ 0 & v_\eta & v_h \end{pmatrix}, \mu = y_s \begin{pmatrix} 1 & 0 & 0 \\ 0 & 1 & 0 \\ 0 & 0 & 1 \end{pmatrix} v_s, M = y_R \begin{pmatrix} 1 & 0 & 0 \\ 0 & 1 & 0 \\ 0 & 0 & 1 \end{pmatrix} v_R. \tag{5.2.4}$$

We notice that, m_D is connected to v_η and v_h, and M is determined by the VEV v_R. In this way, the order of magnitude involved in the Eq. 5.2.2 is such that, $m_\nu \propto \frac{(v_\eta + v_h)^2}{v_R^2}\mu$. Here v_η and v_h are of the order of electroweak breaking, v_R is of the order of TeV scale. Therefore, to get m_ν in sub-eV, μ which is coming from the VEV of Φ_S should be of the order of keV.

Type II seesaw with triplet Higgs

We have chosen type II seesaw for reproducing non-zero θ_{13}. For the implementation of type II seesaw mechanism the SM is extended by the inclusion of an additional $SU(2)_L$ triplet scalar field Δ. Apart having bilinear and quartic terms the triplet also has a trilinear mass term $\mu_{\phi\Delta}$ which generates an induced VEV for the neutral component of the Higgs triplet as $\Delta^0 = v_\Delta\sqrt{2}$ where, $v_\Delta \simeq \mu_{\phi\Delta}v^2/\sqrt{2}M_\Delta^2$ [14–18]. The type II seesaw contribution to light neutrino mass is given by

$$m_{LL}^{II} = f_\nu v_\Delta, \tag{5.2.5}$$

In the low scale type II seesaw mechanism operative at the TeV scale, barring the naturalness issue, one can consider a very small value of the trilinear mass parameter to be

$$\mu_{\phi\Delta} \simeq 10^{-8} GeV.$$

The sub-eV scale light neutrino mass with type II seesaw mechanism constrains the corresponding Majorana Yukawa coupling as

$$f_\nu^2 < 1.4 \times 10^{-5}(\frac{M_\Delta}{1TeV}).$$

Within the reasonable value of $f_\nu \simeq 10^{-2}$, the triplet Higgs scalar VEV is $v_\Delta \simeq 10^{-7} GeV$ which is in agreement with oscillation data. The Yukawa Lagrangian for the type II seesaw part is given by,

$$\mathcal{L}^{II} = f_\nu \frac{LL\zeta\triangle}{\Lambda} + f_\nu \frac{LL\xi\triangle}{\Lambda} \tag{5.2.6}$$

Where, Λ is the cutoff scale. With the type II perturbation the Lagrangian takes the following form

$$\mathcal{L} = y_D \bar{L}\nu_R\eta + y_D{}'\bar{L}\nu_R h + y_M\nu_R S\phi_R + y_s SS\phi_s + f_\nu \frac{LL\zeta\triangle}{\Lambda} + f_\nu \frac{LL\xi\triangle}{\Lambda}. \tag{5.2.7}$$

The first four terms of the above equation are considered to be the leading order contribution, and the last two terms are for the perturbation to generate non-zero θ_{13}. As summarized in the Table 5.1 the $SU(2)_L$ lepton doublets are supposed to transform as S_4 triplets. The $SU(2)_L$ triplet Higgs field Δ_L is supposed to

transform as a S_4 singlet. We have introduced two more flavon fields ξ and ζ which are assumed to transform as 2 and 3_1 of S_4 respectively.
The decomposition of the $\frac{LL\zeta\triangle}{\Lambda}$ term into S_4 singlet with the multiplication rules can be shown as follows

$$LL\zeta\Delta = (L_2L_2' - L_3L_3^{\prime})\zeta_1\Delta$$
$$3_1 \times 3_1 \sim 2$$
$$2 \times 2 \sim 1$$
$$1 \times 1 \sim 1$$

The decomposition of the $\frac{LL\xi\Delta}{\Lambda}$ term into S_4 singlet with the multiplication rules is given by

$$LL\xi\Delta = (-L_2L_1 - L_1L_2 + L_1L_3 + L_3L_1)v_\xi\Delta$$
$$3_1 \times 3_1 \sim 3_1$$
$$3_1 \times 3_1 \sim 1$$

The flavon alignments which help in constructing the m_{LL}^{II} matrix are as follows

$$\Delta \sim v_\Delta,\ <\zeta> \sim \sqrt{2}v_\zeta(1,0),\ <\xi> \sim v_\xi(0,1,-1).$$

ζ and ξ are assumed to take the VEV in the same scale $v_\zeta = v_\xi = \Lambda$. With these flavon alignments the following structure for the type II seesaw mass matrix m_{LL}^{II} is constructed.

$$m_{LL}^{II} = \begin{pmatrix} 0 & -w & w \\ -w & w & 0 \\ w & 0 & -w \end{pmatrix}. \tag{5.2.8}$$

The three matrices (5.2.4) lead to the following leading order light neutrino mass matrix under the ISS framework.

$$m_\nu = y^2 U_\nu m_0^{\text{diag}} U_\nu^T, \tag{5.2.9}$$

where, m_0 is a non-diagonal matrix given by Eq. (5.4.1). The two Yukawa couplings are supposed to have the same numerical value, $y_D = y_D{}' = y$, which

governs the interactions shown by the first two terms in the Eq. (5.2.3). Now the Lagrangian for the charged lepton mass is ,

$$\mathcal{L}^l = y_l \bar{L} l_R \Phi_l + y_l{}' \bar{L} l_R \Phi_l{}' + y_l{}'' \bar{L} l_R \Phi_l{}'', \tag{5.2.10}$$

The following flavon alignments allow us to have the mass matrix corresponding to the charged lepton sector as given by the Eq. (5.2.11).

$$< \Phi_l >= v_l(1,1,1),\ < \Phi_l{}' >= v_l{}'(1,1,1),\ < \Phi_l{}'' >= v_l{}''$$

S_4 product rules and the chosen vev alignments yield the charged lepton mass matrix as follows,

$$m_l = \begin{pmatrix} y_l{}'' v_l{}'' & y_l v_l - y_l{}' v_l{}' & y_l v_l + y_l{}' v_l{}' \\ y_l v_l + y_l{}' v_l{}' & y_l{}'' v_l{}'' & y_l v_l - y_l{}' v_l{}' \\ y_l v_l - y_l{}' v_l{}' & y_l v_l + y_l{}' v_l{}' & y_l{}'' v_l{}'' \end{pmatrix}, \tag{5.2.11}$$

As the charge lepton matrix in non-diagonal, the charge lepton mass matrix m_l is diagonalized by the magic matrix U_ω exhibited in the following equation.

$$U_\omega = 1/\sqrt{3} \begin{pmatrix} 1 & 1 & 1 \\ 1 & \omega & \omega^2 \\ 1 & \omega^2 & \omega \end{pmatrix}, \tag{5.2.12}$$

(with $\omega = \exp 2i\pi/3$). Considering up to leading order ISS, one can write,

$$U_{TBM} = U_l^\dagger U_\nu.$$

where, U_l corresponds to the identity matrix if the charged lepton mass matrix is diagonal. Since in our work, the charged lepton mass matrix is non-diagonal, U_l is nothing but the magic matrix U_ω given by Eq. (5.2.12). Now in the basis, where charged lepton is diagonal

$$U_\nu \to U_{\rm TBM} = U_\omega^\dagger U_\nu,$$

The Eq. (5.2.9) implies that,

$$U_\omega m_\nu U_\omega^{-1} = y^2 U_\omega U_\nu m_o^{\rm diag} U_\nu^T U_\omega^{-1} \implies m_\nu^{\rm TBM} = y^2 U_{\rm TBM} m_o^{diag} U_{\rm TBM}^T. \tag{5.2.13}$$

5.3 Neutrinoless double beta decay

Neutrinoless double beta decay (NDBD) is a process where two protons are converted into two electrons with no neutrinos in the final state, leading to the violation of lepton number by two units.

$$N(A, Z) \rightarrow N(A, Z + 2) + e^- + e^-.$$

This violation of lepton number makes this process a strong probe of Majorana neutrinos [19–22]. The time period of NDBD is dependent on the effective mass m_ν^{ee} as we have already mentioned in Chapter 2. If we recall the effective mass formula it is given by,

$$|m_\nu^{ee}| = |U_{ei}^2 m_i|, \tag{5.3.1}$$

There may have several contributions [23, 24] that influence the effective mass prediction. In this work since we have considered the ISS mechanism to explain tiny neutrino mass, only relevant contribution will come from the process occurred due to SM light neutrino exchanges. On the other hand the contribution from the triplet Higgs is of the order of $10^{-13} m_i$ which is relatively concealed as compared to the dominant contribution [25]. One can determine the effective neutrino mass from the following expression given by,

$$m_{\nu,LL}^{ee} \simeq U_{e1}^2 m_1 + U_{e2}^2 e^{2i\alpha} m_2 + U_{e3}^2 e^{2i\beta} m_3. \tag{5.3.2}$$

From the effective mass formula it is clear that $m_{\nu,LL}^{ee}$ solely depends on the matrix elements of the first row of the $U_{\rm PMNS}$ mixing matrix and the light neutrino mass eigenvalues. The matrix elements are functions of the neutrino mixing angles. Therefore, $m_{\nu,LL}^{ee}$ for the present model under discussion is dependent on the predictions regarding the oscillation parameters, made by the model. At the same time the light neutrino mass eigenvalues are different for different mass hierarchy patterns, normal and/or inverted. This fact clearly indicates that, the effective mass will be different for different mass hierarchy patterns. We evince the plots for effective mass prediction due to SM light neutrino exchanges in figure 5.9.

5.4 Numerical analysis

The global fit neutrino oscillation data used for this work is taken from [26], which is exhibited in Table 5.2.

Oscillation parameters	bfp(NO)	3σ Cl(NO)	bfp(IO)	3σ Cl(IO)
$\Delta m^2_{21}[10^{-5}eV^2]$	7.5	(7.02 , 8.07)	7.5	(7.02 , 8.07)
$\Delta m^2_{31}/\Delta m^2_{23}(NO/IO)[10^{-3}eV^2]$	2.457	(2.317 , 2.607)	-2.449	(-2.590 , -2.307)
$\sin^2\theta_{12}$	0.304	(0.270 , 0.344)	0.304	(0.270 , 0.34)
$\sin^2\theta_{13}$	0.0218	(0.0186 , 0.0250)	0.0219	(0.0188 , 0.0251)
$\sin^2\theta_{23}$	–	0.381-0.643	–	(0.388 , 0.644)

Table 5.2: Gobal fit oscillation data from reference [26]

Each value of y (which is present in the m_D) gives rise to various sets of the neutrino mass matrix parameters a, b.

As shown in [6] that the ISS mechanism also yields some potential way to obtain TBM mixing pattern. In the present analysis, we consider $M \propto I$, $\mu \propto I$ and $m_D \propto M_0$. These three matrices give rise to neutrino mass matrix which is of TBM pattern, that naturally accounts for vanishing θ_{13}. We parameterize the light neutrino mass matrix obtained from the ISS realization with the help of recent neutrino oscillation data given in Table 5.2. Using Eq. (5.2.4) the light neutrino mass matrix is found to be

$$M^0_\nu = y^2 \frac{y_s v_v}{y_R^2 v_R^2} \begin{pmatrix} v_h^2 & 0 & 0 \\ 0 & v_h^2 + v_\eta^2 & 2v_h v_\eta \\ 0 & 2v_h v_\eta & v_h^2 + v_\eta^2 \end{pmatrix}$$

Now, if we define some parameters $a = \frac{\sqrt{y_s v_s}}{y_R v_R} v_h$ and $b = \frac{\sqrt{y_s v_s}}{y_R v_R} v_\eta$ the light neutrino mass matrix can take the following form given by Eq. (5.2.11).

$$M^0_\nu = y^2 \begin{pmatrix} a^2 & 0 & 0 \\ 0 & a^2 + b^2 & 2ab \\ 0 & 2ab & a^2 + b^2 \end{pmatrix} = y^2 m_o, \tag{5.4.1}$$

then we solve for a and b with the help of two mass squared splittings taken from the global fit oscillation data. While finding the solutions for a and b each time

we vary the Yukawa coupling y present in Eq. (5.2.9). For each Yukawa value we get different sets of solutions for a and b. Choosing each set of a, b values and that particular Yukawa coupling chosen for a particular set we get sets of light neutrino mass matrices. Once we get these light neutrino mass matrix, to this we add the type II perturbation matrix to reproduce nonzero θ_{13}. After adding the perturbation we get the neutrino mass matrix as follows,

$$M_\nu = M_\nu^0 + m_\nu^{II} = y^2 U_{TBM} m_\nu^{diag} U_{TBM}^T + m_\nu^{II}.$$

The numerical value of the perturbation term $w = f_\nu v_\Delta$ critically depends upon the Majorana coupling f_ν, trilinear mass parameter $\mu\phi\Delta$ and M. Accordingly, we vary the type II seesaw strength from 10^{-6} to 0.01 eV to produce non-zero θ_{13}. It is observed from the figures 5.1 and 5.2 that the type II seesaw strength of 10^{-3} eV is generating the non-zero θ_{13} in the 3σ range of all the cases. After getting the complete mass matrix we diagonalize it. After diagonalization the mass eigenvalues are found to be $m_1 = y^2a^2$, $m_2 = y^2(a+b)^2$, $m_3 = y^2(a-b)^2$. Now the elements of these diagonalized matrices are associated with the parameters of the model and the type II perturbation term. The set of a, b values obtained for each y value and chosen for analysis are listed in Table 5.3, Table 5.4, Table 5.5 for NH case and Table 5.6, Table 5.7, Table 5.8 for IH case.

Parameters	$y = 0.99$	$y = 0.992$	$y = 0.994$	$y = 0.996$	$y = 0.998$	$y = 1$
a	0.0633626	0.0632349	0.0631076	0.0624	0.0622749	0.062729
b	0.161879	0.161552	0.161227	0.16017	0.159849	0.16026

Table 5.3: Values of a, b obtained by solving for NH case with best fit central value of 3σ deviations

Parameters	$y = 0.99$	$y = 0.992$	$y = 0.994$	$y = 0.996$	$y = 0.998$	$y = 1$
a	0.0641786	0.0640492	0.0639203	0.063792	0.0636641	0.0635368
b	0.164422	0.16409	0.16376	0.163431	0.163104	0.162777

Table 5.4: Values of a, b obtained by solving for NH case with a upper bound of 3σ deviations

Parameters	$y = 0.99$	$y = 0.992$	$y = 0.994$	$y = 0.996$	$y = 0.998$	$y = 1$
a	0.0625069	0.0623809	0.0622554	0.0621304	0.0620059	0.0618818
b	0.159456	0.159135	0.158815	0.158496	0.158178	0.157862

Table 5.5: Values of a, b obtained by solving for NH case with an lower bound of 3σ deviations

Parameters	$y = 0.99$	$y = 0.992$	$y = 0.994$	$y = 0.996$	$y = 0.998$	$y = 1$
a	0.0640348	0.0639057	0.0637771	0.063649	0.0635215	0.0633944
b	0.162732	0.162404	0.162077	0.161752	0.161428	0.161105

Table 5.6: Values of a, b obtained by solving for IH case with best fit central value of 3σ deviations

Parameters	$y = 0.99$	$y = 0.992$	$y = 0.994$	$y = 0.996$	$y = 0.998$	$y = 1$
a	0.0647916	0.064661	0.0645309	0.0644013	0.0642722	0.0641437
b	0.165197	0.164864	0.164533	0.164202	0.163873	0.163545

Table 5.7: Values of a, b obtained by solving for IH case with a upper bound of 3σ deviations

Parameters	$y = 0.99$	$y = 0.992$	$y = 0.994$	$y = 0.996$	$y = 0.998$	$y = 1$
a	0.0631378	0.0630105	0.0628838	0.0627575	0.0626317	0.0625065
b	0.160259	0.159935	0.159614	0.159293	0.158975	0.158656

Table 5.8: Values of a, b obtained by solving for IH case with an lower bound of 3σ deviations

5.5 Results and discussions

A thorough analysis has been carried out to check whether the oscillation parameters are near to reach or not by taking the upper and lower bound of 3σ deviation as well. We fit the values of oscillation parameters using recent cosmological constraints for both normal and inverted mass ordering. We compute all the oscillation parameters also by varying the type II seesaw strength. Variation of type II seesaw strength with the non-vanishing θ_{13}, for both hierarchy patterns have been shown in figure 5.1 using the best fit values and figure 5.2 for the extremum bounds of 3σ deviations. The production of other oscillation parameters, e.g. the two mixing angles and two mass squared splitting as a function of nonzero θ_{13} has been shown in the figure 5.3, figure 5.4 and figure 5.5 for NH case, figure 5.6, figure 5.7 and figure 5.8 for IH case for different values of Yukawa coupling. The sum of absolute masses has also been calculated to see whether it satisfies the Planck upper bound or not. Seeing that, the sum of absolute neutrino masses can give some clue on neutrinoless double beta decay, a little study has been performed to check whether the presented model is able to contribute to the $0\nu\beta\beta$ physics. In figure 5.9 we plot for the contribution of the effective mass to $0\nu\beta\beta$ decay due to light neutrino exchanges for standard contribution. Also the effective mass prediction has been studied varying the type II strength. A comparison among the various sets of results has been shown in the Table 5.9. From the results obtained as clear from the plots 5.1-5.8, we can get the following observations.

- The Yukawa coupling is varied from 0.992 to 1 which is demanded by the neutrino parameters to being in their allowed 3σ range.

- The non-zero value of θ_{13} has been found to be consistent with the variation of type II seesaw strength for both kinds of hierarchy patterns.

- The proposed model is able to evince a good neutrino phenomenology within the NH framework while taking into consideration the lower bound of 3σ deviation. All the oscillation parameters have been obtained within the correct 3σ range for any value of Yukawa coupling ranging from 0.992

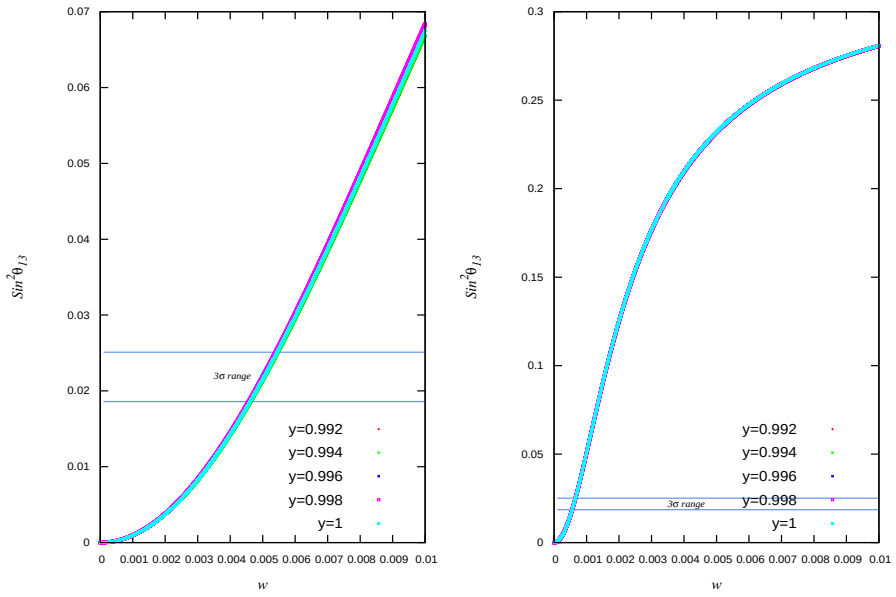

Figure 5.1: Generation of non-zero $sin^2\theta_{13}$, varying the type II strength for best fit mass squared splittings for NH (left panel) and IH (right panel) case.

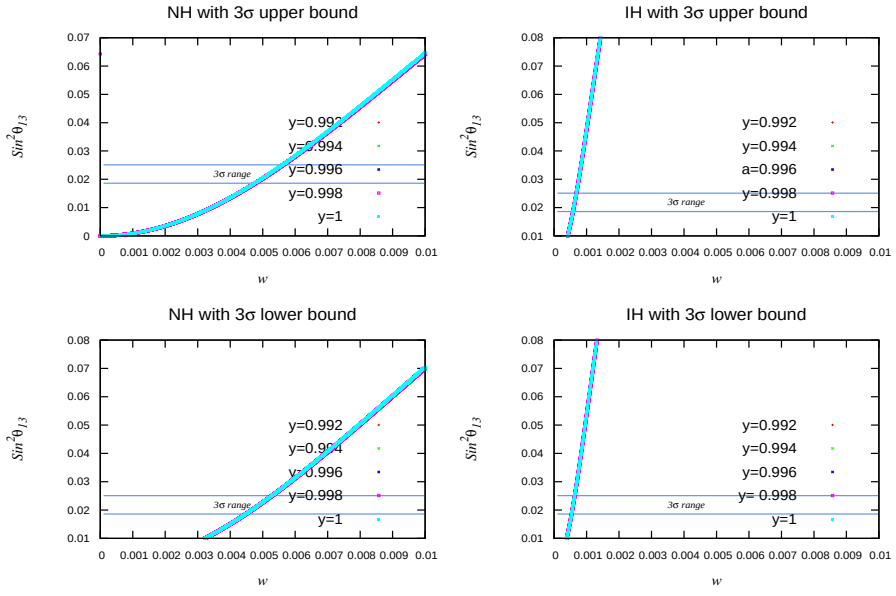

Figure 5.2: Generation of non-zero $sin^2\theta_{13}$, varying the type II strength using lower and upper bound of 3σ deviations.

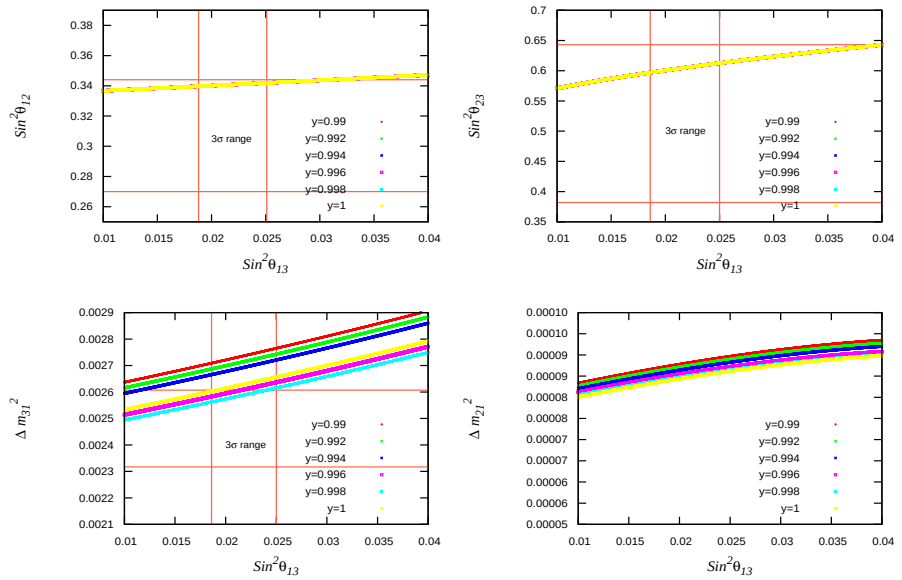

Figure 5.3: Variation of $sin^2\theta_{12}$, $sin^2\theta_{23}$,Δm^2_{31} and Δm^2_{21} with $sin^2\theta_{13}$ for NH case with best fit values

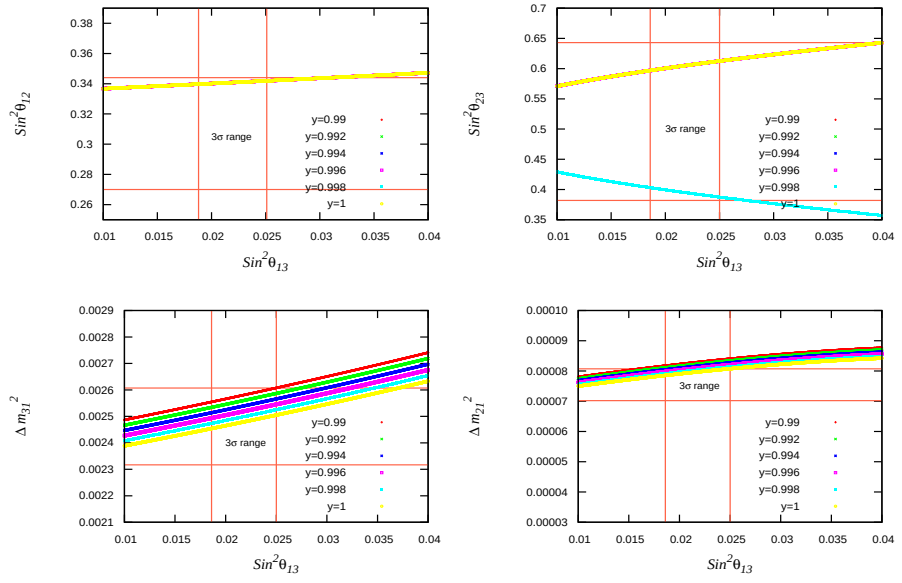

Figure 5.4: Variation of $sin^2\theta_{12}$, $sin^2\theta_{23}$,Δm^2_{31} and Δm^2_{21} with $sin^2\theta_{13}$ for NH case with lower bound of 3σ deviation

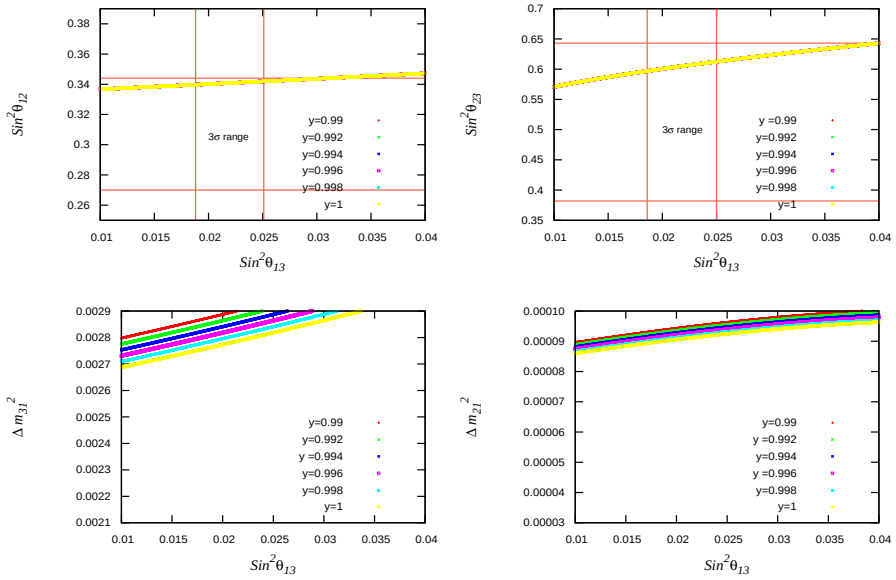

Figure 5.5: Variation of $sin^2\theta_{12}$, $sin^2\theta_{23}$,Δm^2_{31} and Δm^2_{21} with $sin^2\theta_{13}$ for NH case with with upper bound of 3σ deviation

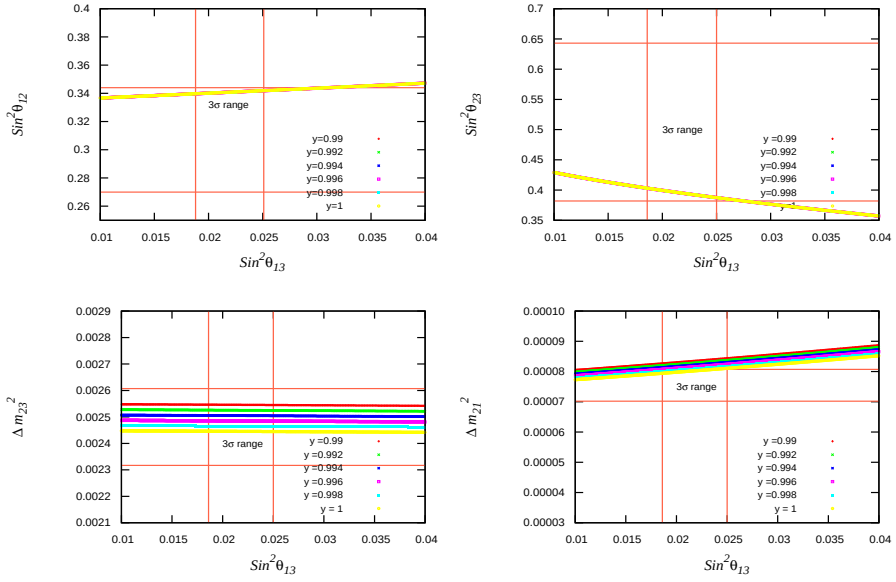

Figure 5.6: Variation of $sin^2\theta_{12}$, $sin^2\theta_{23}$,Δm^2_{23} and Δm^2_{21} with $sin^2\theta_{13}$ for IH case with best fit value

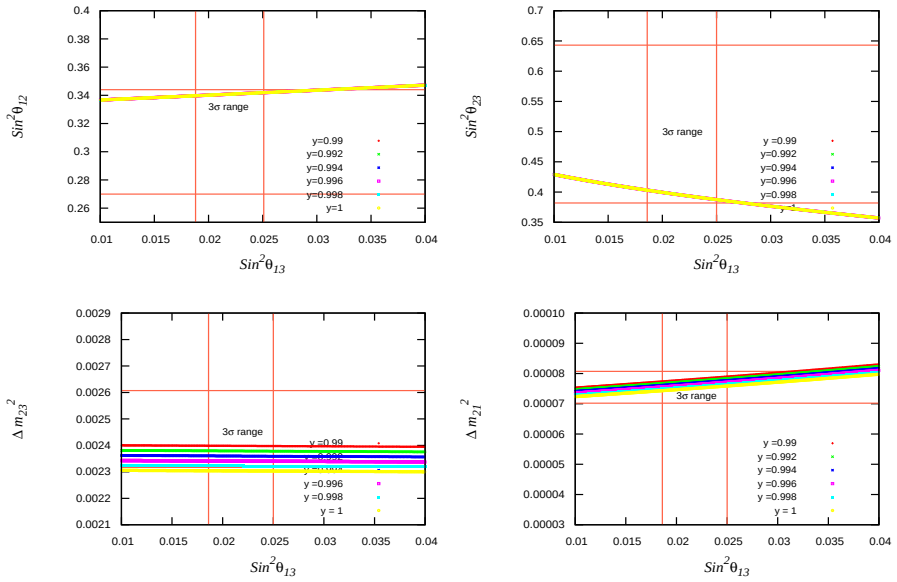

Figure 5.7: Variation of $sin^2\theta_{12}$, $sin^2\theta_{23}$,Δm^2_{23} and Δm^2_{21} with $sin^2\theta_{13}$ for IH case with lower bound of 3σ deviation

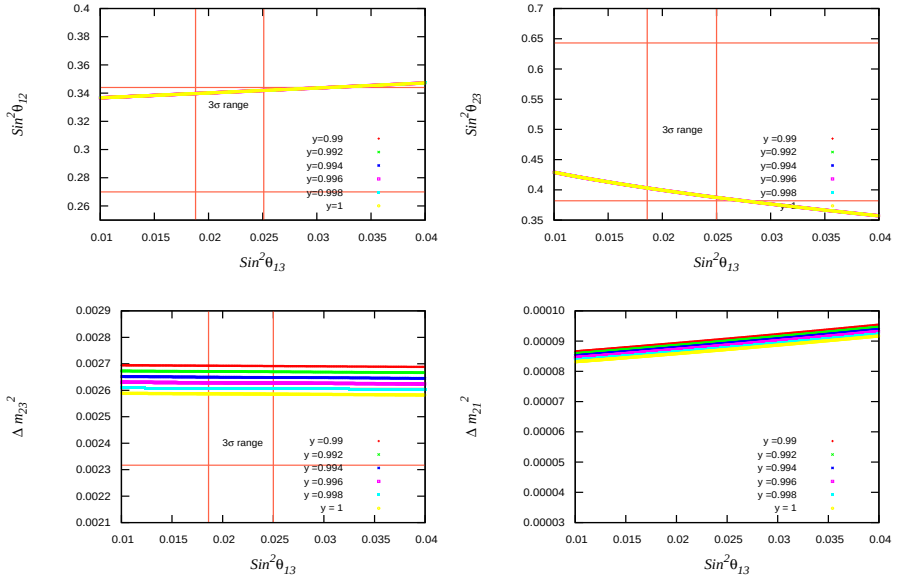

Figure 5.8: Variation of $sin^2\theta_{12}$, $sin^2\theta_{23}$,Δm^2_{23} and Δm^2_{21} with $sin^2\theta_{13}$ for IH case with upper bound of 3σ deviation

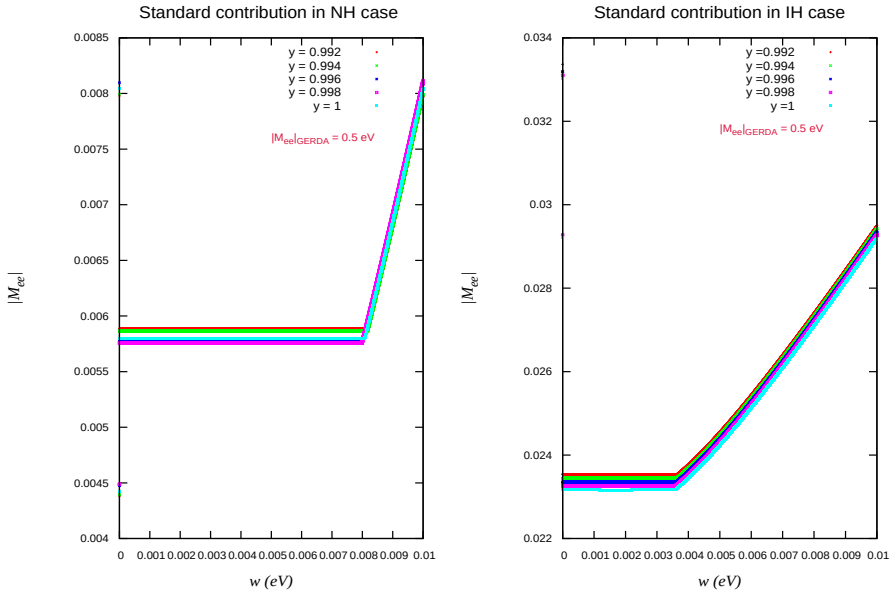

Figure 5.9: Variation of effective mass $|M_{ee}|$ (in eV)for the standard and non-standard contribution to $0\nu\beta\beta$ decay due to light neutrino exchanges [27].

to 1 for NH case. Taking the best fit value and the upper bound of 3σ deviation for NH case, the model is found to be unable to produce Δm^2_{21} and Δm^2_{31} within the correct 3σ range.

- It has been noticed that the proposed model also shows evidences for correct neutrino phenomenology using the best fit and lower 3σ bound for mass squared splittings in case of inverted hierarchy mass pattern.

- The effective mass predictions for $0\nu\beta\beta$ decay for both NH and IH are obtained in the vicinity of experimental results as shown in figure 5.9.

5.6 Conclusion

We have studied an S_4 based ISS model which is accompanied by the type II seesaw as a perturbation to the leading order ISS mass, from the need of bringing non vanishing reactor angle into account. We have chosen one ISS scheme among the seven schemes as listed by the authors in [6] and extended the study to a search for $\theta_{13} \neq 0$. The entire study has been performed from a different aspect;

Model	θ_{13}	θ_{12}	θ_{23}	Δm^2_{21}	$\Delta m^2_{31}, \Delta m^2_{23}$	$\sum_{i=1,2,3} \mod m_i$
NH (bfp)	✓	✓	✓	×	✓	✓
NH (lower 3σ bound)	✓	✓	✓	✓	✓	✓
NH (upper 3σ bound)	✓	✓	✓	×	×	✓
IH (bfp)	✓	✓	✓	✓	✓	✓
IH (lower 3σ bound)	✓	✓	✓	✓	✓	✓
IH (upper 3σ bound)	✓	✓	✓	×	✓	✓

Table 5.9: Summary of results obtained from various allowed mass schemes.

by extracting the Yukawa coupling (y) from the light neutrino mass matrix and varying it from and to a certain range, in order to check the parameter space of the Yukawa coupling strength and the global fit neutrino parameters. For NH mass pattern it is seen that only the lower bound of the mass squared splittings can give a solution for the model parameters $a,\ b$ who further give rise to the other oscillation parameters in correct 3σ range for the chosen range of Yukawa coupling (y). For the same Yukawa coupling range the model prediction is more sensitive to IH mass pattern, as we obtain the oscillation parameters in agreement with experiments, while scanning the mass squared splittings from the lower bound of the 3σ bound to the best fit central value. Thus, we can conclude that a broader region of parameter space exists in case of IH. From the type II seesaw term we have the type II strength w which reproduces non-zero θ_{13} in the correct 3σ range. We have also studied the effective mass prediction for the contribution of NDBD. However, for both hierarchy pattern we get the effective mass within GERDA limit [27]. The variation of Yukawa coupling makes a better plot for a detailed study of the neutrino parameters. As we also have some complex solution for the model parameters a, b, considering them we can further go for lepton asymmetry study (by considering a non-degenerate M structure), as the complex nature of a, b may be a source of CP violation. The complex solutions of a, b almost yield the same neutrino phenomenology. Moreover, this study of variation of Yukawa coupling may have some effect on the order of lepton asymmetry that can account for the observed matter-antimatter asymmetry.

Bibliography

[1] Abe, K. et al. Indication of Electron Neutrino Appearance from an Accelerator-produced Off-axis Muon Neutrino Beam, *Physical Review Letters*, 107(4):041801, 2011.

[2] Ahn, J. K., et al. Observation of Reactor Electron Antineutrinos Disappearance in the RENO Experiment. *Physical Review Letters*, 108(19):191802, 2012.

[3] An, F. P., et al. Observation of electron-antineutrino disappearance at Daya Bay. *Physical Review Letters*, 108(17):171803, 2012.

[4] Weinberg, S. Baryon and Lepton Nonconserving Processes. *Physical Review Letters*, 43(21):1566, 1979.

[5] Babu, K.S., Leung, C. N., and Pantaleone, J. T. Renormalization of the neutrino mass operator. *Physics Letters B*, 319:191, 1993.

[6] Hirsch, M., Morisi, S. and Valle, J. W. F. A_4 based tri-bimaximal mixing within inverse and linear seesaw schemes. *Physics Letters B*, 679:454-459, 2009.

[7] Mohapatra, R. N. and Valle, J. W. F. Neutrino mass and baryon-number nonconservation in superstring models. *Physical Review D*, 34(5):1642-1645, 1986.

[8] Mohapatra, R. N. Mechanism for Understanding Small Neutrino Mass in Superstring Theories. *Physical Review Letters*, 10(6):56, 1986.

[9] Dias, A. G., de S. Pires, C. A., and da Silva, P. S. R. How the inverse seesaw mechanism can reveal itself natural, canonical, and independent of the right-handed neutrino mass. *Physical Review D*, 84(5):053011, 2011.

[10] Dias, A. G. , de S. Pires, C. A., da Silva, P. S. R., and Sampieri, A. A Simple Realization of the Inverse Seesaw Mechanism. *Physical Review D*, 86(3):035007, 2012.

[11] Ma, E. Radiative inverse seesaw mechanism for nonzero neutrino mass. *Physical Review D*, 80(1): 013013, 2009.

[12] Dev, P. S. B. and Mohapatra, R. N. TeV scale inverse seesaw model in SO(10) and leptonic nonunitarity effects. *Physical Review D*, 81:013001, 2010.

[13] Ishimori, H., Kobayashi, T., Ohki, H., Shimizu, Y., Okada, H., and Tanimoto, M. Non-Abelian Discrete Symmetries in Particle Physics. *Progress of Theoretical Physics Supplement*, 183:1, 2010

[14] Mukherjee, A. and Das, M. K., Neutrino phenomenology and scalar Dark Matter with A_4 flavor symmetry in Inverse and type II seesaw, *Nuclear Physics B*, 913:643-663, 2016.

[15] Borah, M., Borah, D., Das, M. K., and Patra, S. Perturbations to the $\mu-\tau$ symmetry, leptogenesis and lepton flavor violation with the type II seesaw mechanism. *Physical Review D*, 90(9):095020, 2014.

[16] Rodejohann, W. Type II See-Saw Mechanism, Deviations from Bimaximal Neutrino Mixing and Leptogenesis. *Physical Review D*, 70(7):073010, 2004.

[17] Lindner, M. and Rodejohann, W. Large and Almost Maximal Neutrino Mixing within the Type II See-Saw Mechanism. *Journal of High Energy Physics*, 05:089, 2007.

[18] Borah, D. Deviations from tri-bimaximal neutrino mixing using type II seesaw. *Nuclear Physics B*, 876(2):575-586, 2013.

[19] Rodejohann, W., Neutrino-less double beta decay and particle physics. *Internatinonal Journal of Modern Physics E* , 20(09):1833, 2011.

[20] Klapdor-Kleingrothaus, H. V., Dietz, A., Harney, H. L., and Krivosheina, I. V. Evidence for neutrinoless double beta decay. *Modern Physics Letters A*, 16:2409, 2001.

[21] Bilenky,S. M. and Giunti, C. Neutrinoless double beta decay: A brief review. *Modern Physics Letters A*, 27(13):1230015, 2012.

[22] Vergados, J.D., Ejiri, H., and Simkovic, F. Theory of Neutrinoless Double Beta Decay. *Reports on Progress in Physics*, 75:106301, 2012.

[23] Borah, D. and Dasgupta, A. Charged lepton flavour violation and neutrinoless double beta decay in left-right symmetric models with type I+II seesaw. *Journal of High Energy Physics*, 07:022, 2016.

[24] Borgohain, H. and Das, M. K. Neutrinoless double beta decay and lepton flavour violation in broken $\mu - \tau$ symmetric neutrino mass models. *International Journal of Theoretical Physics* , 56(9): 2911, 2017.

[25] Chakrabortty, J., et al. Neutrinoless double-Îš decay in TeV scale left-right symmetric models. *Journal of High Energy Physics*, 08:008, 2012.

[26] Bergstrom, J., Gonzalez-Garcia, M. C., Maltoni, M., and Schwetz, T. Bayesian Global analysis of neutrino oscillation data, *Journal of High Energy Physics*, 1509:200, 2015.

[27] Agostini, M., et al. Search of Neutrinoless Double Beta Decay with the GERDA Experiment. In *37th International Conference on High Energy Physics (ICHEP 2014)*, volumes(273-275), pages 1876-1882, Valencia, Spain, 2-9 Jul 2014. Elsevier.